Temporal and spatial evolution of Si atoms in plasmas produced by a nanosecond laser ablating silicon carbide crystals

Ming Chen,[1] Xiangdong Liu,[1,2,*] Mingwen Zhao,[1,2] Chuansong Chen,[3] and Baoyuan Man[3]
[1]*School of Physics, Shandong University, Jinan 250100, China*
[2]*State Key Laboratory of Crystal Materials, Shandong University, Jinan 250100, China*
[3]*College of Physics and Electronics, Shandong Normal University, Jinan 250014, China*
(Received 10 April 2009; revised manuscript received 9 June 2009; published 13 July 2009)

Optical emission spectroscopy (OES) was used to study the evolution behavior of the neutral Si atoms in the plasma produced by nanosecond pulsed-laser beam irradiating on SiC crystal targets. The OES measurements indicated that the electron temperature and density in the plasma had maximum values around a region about 2mm from the target surface. Based on the temporal and spatial evolution of the spectral line at 633.19 nm originating from excited Si atoms, it was found that these Si atoms have short decay times and long range spatial distribution in vacuum. At the initial growth stage of SiC thin films using pulsed-laser deposition (PLD) technique, these Si atoms were found possibly to arrive at the Si substrate to form defects near the SiC/Si interface. By comparing the OES result measured in vacuum and that measured in ambient air, it was deduced that by properly adjusting the background gas species and pressure, the quality of the films prepared by PLD technique may be improved.

DOI: 10.1103/PhysRevE.80.016405 PACS number(s): 52.38.Mf, 52.70.−m

I. INTRODUCTION

Pulsed-laser ablation of solids has long been used as a unique technique to deposit high-quality films [1–3] for variety of applications, such as production of circuit components with superconducting or insulating properties, wearing resistance films, and biocompatible devices for medical application [2–8]. Among various films prepared using pulsed-laser deposition (PLD) method, silicon carbide (SiC) thin films have great advantage for applications in electronic devices working at high-power level, biocompatible material or devices, and microelectromechanical systems due to their large electronic band gaps, superior mechanical strength and durability, and radiation-resistant property [9–11]. However, higher density of defects such as droplets, stacking faults, and dislocations are frequently observed in the SiC films prepared on Si substrates by using PLD method, in comparison with those prepared by using chemical vapor deposition (CVD) or supersonic jet epitaxy (SJE) [12–15]. At early deposition stage, Si atoms have higher probability to recrystallize epitaxially on Si substrate than carbon atoms. This makes it difficult to transfer adequate amounts of silicon atoms and carbon atoms in accordance with the chemical stoichiometry of SiC [14,15]. Due to this recrystallization process, the defects produced at the SiC/Si interface and in the SiC film will greatly degrade the performance of the optoelectronics devices made from PLD films [16]. Therefore, it is absolutely necessary to study the basic physical process involved in deposition of thin films using PLD method to improve the quality of the films prepared.

Basic interactions involved in the plasma produced by laser ablation of SiC material, which is essential for determination of the experimental parameters such as the intensity of the laser beam, the pressure of the background gas, and the spatial position of the substrate relative to the target, to be used in preparation of PLD SiC films. In order to provide information on these processes, the plasma parameters (temperature, density) and relevant physical processes such as the transferring of Si atoms and ions from the target to the substrate, and the interactions between these particles in the plasma and the ambient atmosphere are investigated in this work. It is well known that the plasma emission spectroscopy (PES) is one of the most important techniques to characterize laser-ablated plasma, which contains a wealth of information about the inner plasma condition [1–6]. In this paper, we use this method to study the spatial and temporal evolutions of Si atoms and ions as plasma expanding in background gas media (one atmosphere) and in low-vacuum environment. The aim of this work is to get an insight into the behavior of Si atoms in the laser-ablated SiC plasma.

II. EXPERIMENTAL SETUP

The plasma was produced in vacuum (2.7 Pa) and in air (10^5 Pa), respectively, by ablating a SiC target with the laser pulses from a Nd:YAG (Yttrium Aluminum Garnet) laser (Quanta Ray, Spectra Physics) operating at wavelengths of 1064 nm, with pulse width of 10 ns. The laser beam was focused on the target by a quartz lens (L1) with a 65 mm focal length, and another 50mm quartz lens was used to image the laser-induced plasma 1:1 onto the 15-μm-wide entrance slit of a spectrometer (spectrapro2300i, Actron Research) system. The visible emission image of the plasma plume, as shown in Fig. 1(a), was recorded by a digital camera in vacuum condition. A 1200/mm grating blazed at 500 nm was employed to disperse the plasma. The temporal spectra were detected by using a time-gated intensified charge-coupled device (ICCD) chip (1024×1024 pixels) at various time delays with respect to the ablating laser pulse. The spatial emission lines were measured by another charged-coupled device (CCD) chip (700×1340 pixels) at different

*Corresponding author; xdliu@sdu.edu.cn

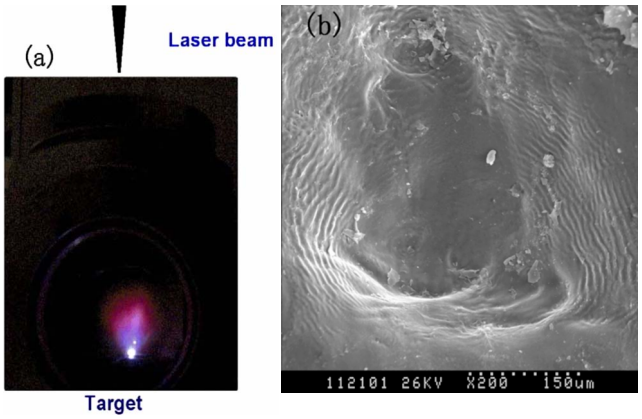

FIG. 1. (Color online) (a) The spatial profile of the visible emission recorded by a digital camera from the plasma produced by nanosecond (10ns) pulsed-laser irradiation on a SiC target; (b) The scanning electron microscopy (SEM) image of a crater formed by 100 laser pulses at 30mJ from a *Q*-switched YAG laser irradiating on a SiC crystal target. The image size of Fig. 1(a) is 5 cm×10 cm.

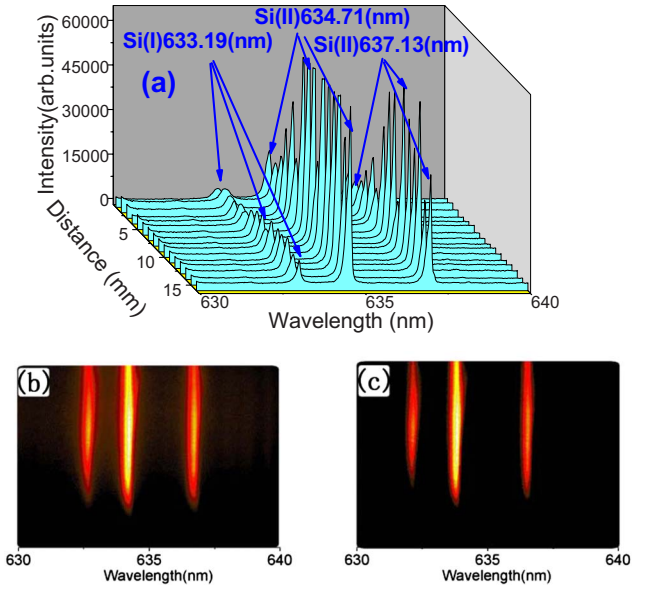

FIG. 2. (Color online) (a) The spatial distribution of the spectra emitted from Si atoms and ions in the plasma measured in a region spanning from the target surface to the edge of the plume; (b) and (c) the images of the emission from Si atoms and ions taken at distance 2 and 8 mm from the target surface, respectively.

distance to the target surface. The grating (minimum gate width of 2ns) ICCD chip and the time integrated CCD chip provide sensitive detection of the plasma spectra in a wavelength range from 200 to 900 nm. The energy of the laser pulses at the target surface was set at a fixed value of 130 mJ, which was monitored by an energy meter (Molectron, EPM1000) in front of the focusing lens L1. The average spot size of the laser beam at the surface of the target was measured to be 1mm in diameter. The incident power density was approximately 1.64 GW/cm^2, which was determined from the energy of the incident laser pulse, the width of the laser pulse and the spot size. To keep a fresh pitting on the target surface, after each laser pulse the target was properly rotated around an axis parallel to the laser beam.

III. RESULTS AND DISCUSSION

The typical surface profile of a crater on the surface of the silicon carbide sample produced by 100 laser pulses was characterized by scanning electron microscopy (SEM) (Philips XL 30 FEG) and is shown in Fig. 1(b). From the SEM image, it is evident that the crater produced by the laser ablation has a circular and periodic wave-like pattern with rather smooth surface in the center of the crater, as shown in Fig. 1(b). This pattern is similar to those observed for the craters created by laser ablation [6]. Energy dispersive x-ray (EDX) spectrum (not shown here) confirms that the elemental ratio of Si to C in the crater is about 16.23%, which essentially deviates from the stoichiometry of SiC. This result suggests that the number of Si species (Si atoms and Si ions) in the plasma is much larger than that of C species. This feature will have important effect on the subsequent deposition of the film.

Figure 2(a) shows three well-isolated lines, emitted by the plasma in vacuum, from Si atoms (at 633.19 nm) and single-charged Si ions (at 634.71 and 637.13 nm), respectively, which were detected at different distance from the target by using time integrated CCD chip. The spectral lines of multi-charged Si ions, such as emissions from double-charged Si ions at 254.18 nm and from triple-charged Si ions at 433.85 and 434.14 nm were also observed in our experiment. However, the intensities of these spectral lines are much lower than that emitted from the neutral Si atoms or single-charged Si ions under the same experimental condition and some of these spectral lines are likely interfered by lines from other species. So in this paper, we only use the representative spectral lines of Si atoms and single-charged Si ions. Along the direction perpendicular to the target surface, it is clearly that the spatial intensity distribution of the line from Si atoms at 633.19 nm nearly extends over the whole spanning distance from the target surface to the edge of the plume (16 mm). The spatial images of the emission from Si atoms and ions at distance 2 and 8 mm from the target surface are clearly shown in Figs. 2(b) and 2(c), respectively. The spectral line from Si atoms at 633.19 nm with long-range spatial distribution indicates that neutral Si atoms ablated from the target can arrive at the substrate and recrystallize on the Si substrate, and thus significantly degrade adhesive strength of the SiC film deposited by PLD method. In addition, some microscopic droplets may also be formed in the film. Before further discussing the characterization of the PES line of neutral Si atoms at 633.19 nm, the plasma parameters, electronic temperature, and density are studied to find out the best spatial location where the electron density and temperature are more suitable for studying the temporal evolution of the spectrum.

Under the assumption of local thermodynamic equilibrium (LTE), the intensities of a set of isolated lines from the ionization states of the same element are used to evaluate the electron temperatures, which is well-known Boltzmann plot method [17,18].

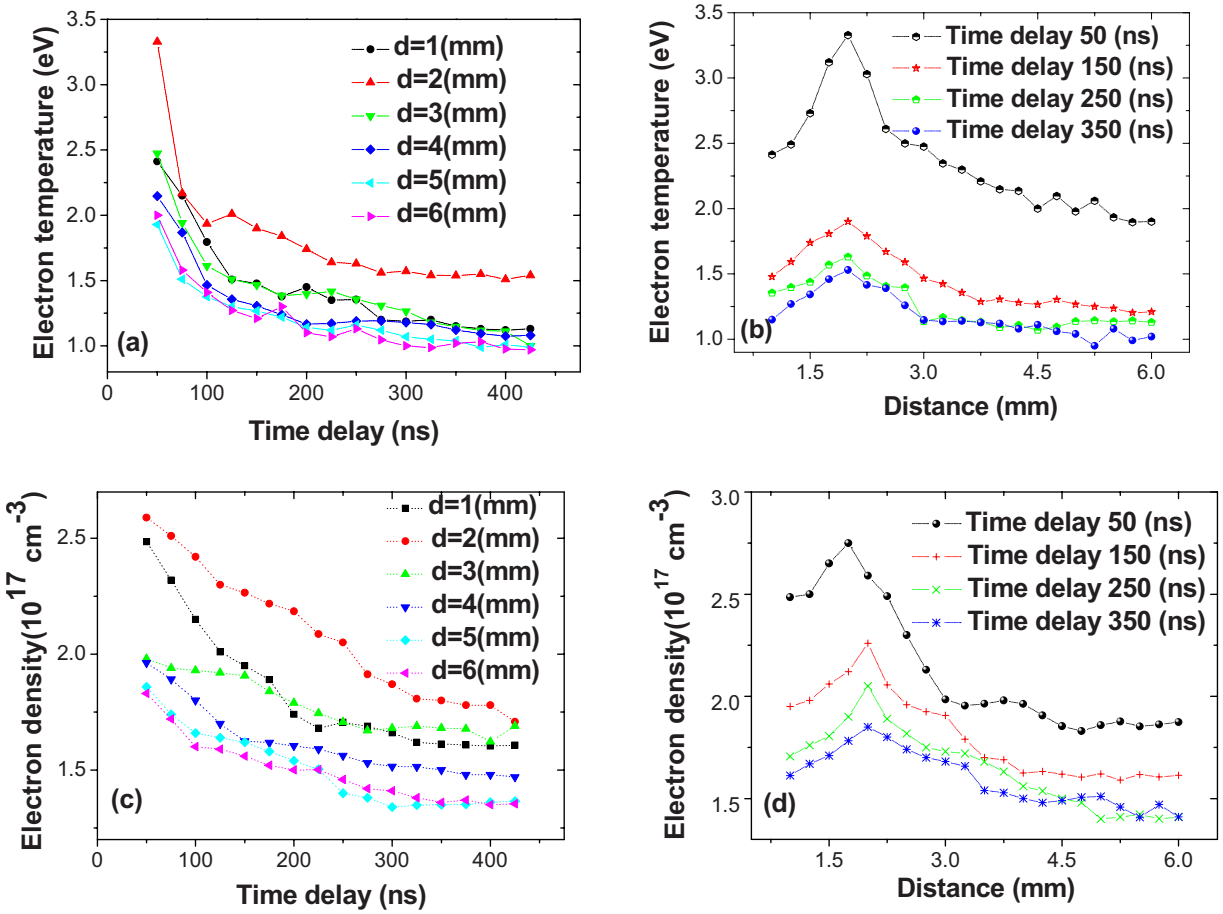

FIG. 3. (Color online) (a) and (b) The temporal evolution of electron temperature and density of the expanding plasma measured at six different distances to the target surface; (b) and (d) show the spatial distribution of the electron temperature and density measured at different delay times with respect to the ablating laser pulse.

$$\ln(I\lambda/Ag_m) = -E_m/kT_e + B, \quad (1)$$

where I, λ, and A refer to the relative integrated intensity, the wavelength and the spontaneous emission rate, respectively, g_m is the statistical weight factor for the excited state, E_m is the energy of the excited state, k is the Boltzmann constant, and B is a constant parameter for all ion lines considered. In this work, the selected emission lines are those at 637.13, 634.71, 413.09, and 412.81 nm, emitted from Si ions. The spectroscopic constants of these spectral lines, such as the central wavelength of emission from individual species, the energy level of the upper states, the absorption oscillator strengths, and the statistical weights of the levels can be found in Ref. [19].

Additionally, the electron density N_e in the plasma can be calculated directly from the measured $\Delta\lambda_{1/2}$ [20], the full width at half maximum (FWHM) of Stark broadening of the spectral line, [17,18,21,22]

$$N_e = \left(\frac{\Delta\lambda_{1/2}}{2W}\right) \times 10^{16}\ \text{cm}^{-3}, \quad (2)$$

where W is an electron impact half width, which is weakly related to temperature. For the evaluation of N_e, in the present work, the Stark broadened FWHM of Si ions at 634.71nm was used. We used W=0.0982 nm for the temperature in a range of 40000–80000 K[22].

To demonstrate the temporal evolution of the electron temperature in vacuum, we measured the spectral images with a constant gate width (t=10 ns) but different delay times (10–600 ns) with respect to the laser pulse. In the early stage, continuum emission dominates the emission spectra with the emission lines overlapping the continuum [1]. Therefore the electron temperature, T_e, were calculated based on the measurements at 50 ns after the ignition of the plasma. Figure 3(a) shows the experimentally measured electron temperature as a function of the delay time at different distance from the target along the propagating direction of the plasma. The curves of electron temperature T_e versus delay time show a very similar behavior for all the detection distances from the target surface. The electron temperature, T_e, decreases substantially with delay time for delay time less than 125 ns. However, for the delay time longer than 125ns, T_e decreases very slowly with increasing of time for the later stage of plasma expansion process (up to 425 ns). Under the same experimental condition, the electron density N_e as a function of the delay time is exhibited in Fig. 3(c). The density decreases in short delay time region (150 ns) and gradually tends to constant density for the later stage of plasma expanding. The measured electron temperature and

density in this paper are in consistent with a recent calculated result (for 10ns laser pulse) [20] using gas-dynamic method to study the laser plasma expansion. The steady behavior of T_e and N_e at the late stage of plasma expansion can be interpreted in accordance with the mechanism of energy release caused by recombinations and bresstrahlung radiation within the plasma, which was proposed by Beilis, Saji, and Harilal [4,5,20]. As shown by Figs. 3(b) and 3(d), the electron temperature and density change substantially as the distance changing from 1 to 6mm for the delay time varying from to 350ns. It is noteworthy that the electron temperature and density first increases up to a maximum at a distance of 2 mm from the target surface, and then cools down slowly for further increase in the distance. The dependence of T_e and N_e on the distance from the target surface within 350 ns clearly indicates that the maximal value of T_e locates at the region about 2 mm from the target surface. As shown in Fig. 2(a), the spatial distribution of the spectral line at 634.71 nm emitted from Si ions in the plasma has relatively large radiation intensity at distance larger than 5mm. However, in contrast to the sharper and higher line distributions at distance larger than 5mm, the line distributions are broader around distance of 2mm from the target surface, where the electron density and temperature are higher than other regions. Our results of the spatial profiles of T_e and N_e as a function of the distance are in consistent with that of a recent study on laser ablation of aluminum targets [21], although the laser intensity used in Ref. [21] was lower than that used in our experiment, their measured T_e was lower than ours and the maximal values of T_e and N_e were approximately located at 1 mm from the target surface.

From the results given above, it suggests that the region around 2 mm from the target surface is the best location for studying the temporal evolution of the spectrum of Si atoms during the plasma expanding process since around where the electron density and temperature are higher than other places.

The calculation of the electron temperature was carried out under the assumption that the plasma was in LTE [17,21,22]. A necessary condition for LTE to be satisfied is [22]

$$N_e \geq 1.4 \times 10^{14} T_e^{1/2} (\Delta E_{\mathrm{mn}})^3 \ \mathrm{cm}^{-3}, \tag{3}$$

where N_e, T_e are the electron density and temperature, respectively. ΔE_{mn} is the energy difference between the upper and the lower energy level in eV. In the present work, the energy level difference for Si ions at 412.807 nm is $\Delta E_{\mathrm{mn}} = 3.01$ eV and the highest electron temperature is 3.32 eV. The lowest limit for N_e can therefore be evaluated using Eq. (3), which is $\sim 6.9 \times 10^{15}$ cm^{-3}. In this study, the average value of electron density changing from 1.35×10^{17} cm^{-3} to 2.59×10^{17} cm^{-3}. The N_e values calculated from our experimental measurement are much higher than the lowest value deduced using Eq. (3). This means that LTE holds true under our experimental condition, and thus the T_e values given in this work are reliable.

To provide crucial information for optimizing the experimental parameters for growing SiC thin film using PLD technique, we also studied the time evolution of the neutral Si atoms in the plasma. Figure 4 shows the emission spectra and the plume images of Si atoms and ions at different delay time (gate width of 5 ns) measured at 2 mm from the target surface in vacuum and air, respectively. It is interesting to see that in vacuum, the time scales ($\sim$175 ns) of the line at 633.19 nm from Si atoms are much shorter than those ($\sim$430 ns) for Si ions at 634.71 and 637.13 nm [Fig. 4(a)]. Figure 4(b) shows the spectra measured in air obtained using similar laser irradiation condition as that used in vacuum. In order to get clearly comparison, the same delay time regions were selected in Figs. 4(a) and 4(b), although the spectral lines of Si ions in air have be detected at 14280 ns delay time. In this case the emission intensity of spectral lines around 633.19 nm are too weak to be detected any more in air [Fig. 4(b)]. The temporal images of the emission from Si atoms and ions are also recorded at delay time of 80 ns, with respect to the ablating laser pulse, in vacuum [Fig. 4(c)] and in air [Fig. 4(d)], respectively. These results clearly reveal that in the plasma ignited by nanosecond pulsed-laser on SiC target, the Si atoms with high density only exist in very early stage of the plasma evolution. Since the spectral line of Si atoms at 633.19 nm disappears only in air environment but not in vacuum, the depopulation of excited Si atoms is due to significant collisions with other particulates in the plasma and with the species relevant to ambient medium, rather than spontaneous emission. Moreover, it is reasonable to deduce that more population of other ions or atoms can be produced due to the energy transfer involved in these intense collisions, which occur in early stage of the plasma expansion. As expected, the signal intensity of spectral line at 637.13 nm originating from Si ions in air medium is almost a factor of 5 larger than that measured in vacuum, as shown in Figs. 4(a) and 4(b). Furthermore, the collisions between Si atoms and ions are enhanced due to the pressure of laser supported denotation (LSD) wave in the ambient medium, and thus the lifetimes of Si ions are largely extended to thousands ns ($\sim 1.428 \times 10^4$ ns) in air medium, which is about 33.2 times longer than that in vacuum ($\sim$430 ns). The pressure delivered to a surface for laser ablation in the atmosphere can be represented by the LSD wave and a combustion wave just above the plasma ignition threshold [23–25]. Once the LSD wave was initiated, almost all of the incident laser energy was absorbed by the LSD wave and the evaporating was soon extricated, although the evaporation wave might exert a very high pressure on the surface at the early stage of the laser pulse. Therefore the pressure and the laser energy delivered to the surface during the plasma expanding process are dominated by the LSD wave. Based on isentropic flow relationships and hydrodynamic shock description of the LSD wave, the pressure, P_D, at the surface induced by the LSD wave can be derived [23–25]:

$$V_D = \left[\frac{2(\gamma^2 - 1) I_0}{\rho_0} \right]^{1/3}, \tag{4}$$

$$P_D = \left[\frac{(\gamma + 1)}{2\gamma} \right]^{2\gamma/\gamma - 1} \frac{\rho_0 V_D^2}{\gamma + 1}, \tag{5}$$

where γ and ρ_0 are the ratio of specific heats of the air behind the detonation wave and the initial mass density of

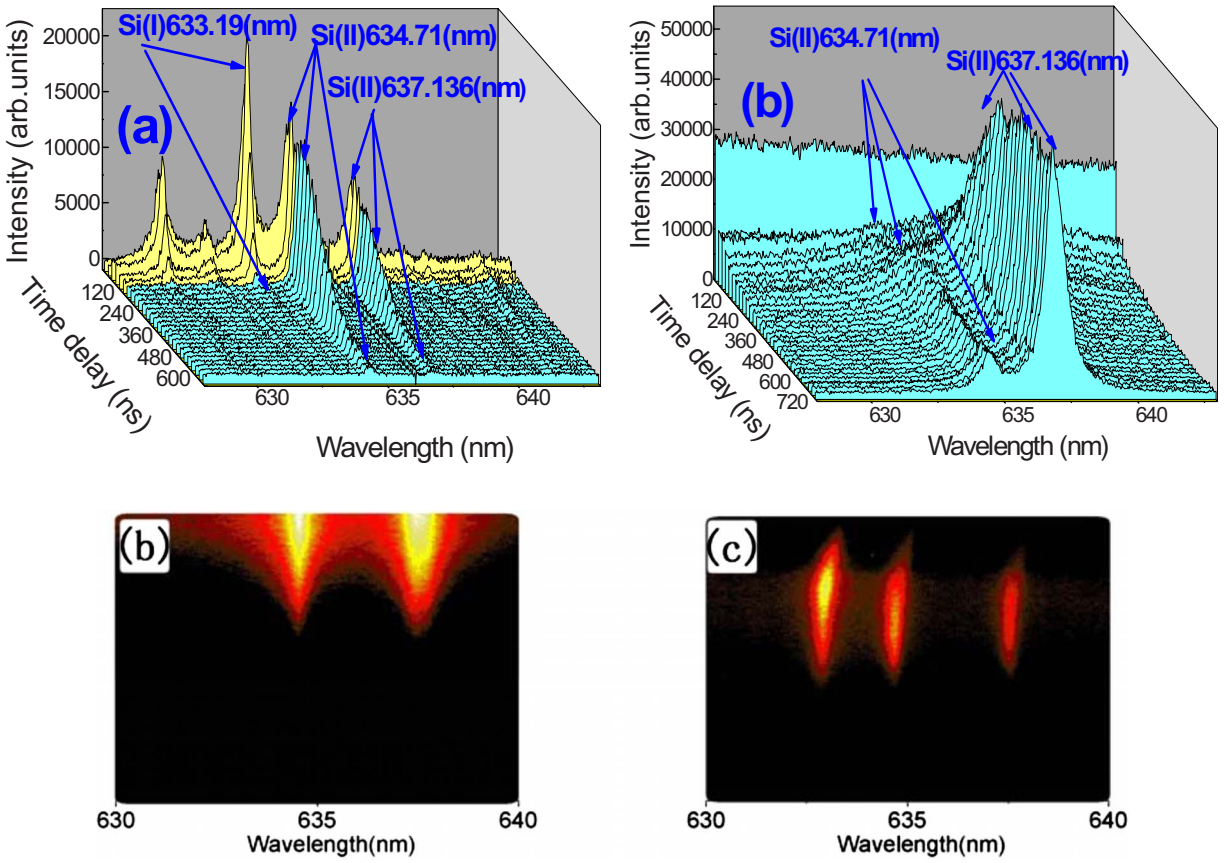

FIG. 4. (Color online) The intensity of the emission spectra from Si atoms and ions versus delay time (gate width of 5 ns), measured at 2 mm from the target surface, (a) measured in vacuum, and (b) measured in air. The images of the emission from Si atoms and ions at delay time of 80 ns recorded (c) in vacuum, and (d) in air, respectively.

the ambient air, respectively, and I_0 is the laser irradiance. Using the values of $\gamma=1.21$, $\rho_0=1.27\times10^{-3}$ g cm^{-3} for ambient at 1 atmosphere, and the laser intensity $I_0=1.64$ GW/cm^2 used in our experiment, from Eqs. (4) and (5) we estimated the pressure delivered to the surface by the LSD wave, which is $\sim1.06\times10^8$ Pa in ambient air. However, under the vacuum condition (2.7 Pa in our experiment), the mass density of the residual air decreases to $\sim3.42\times10^{-8}$ g cm^{-3}. In contrast to the significant drop of mass density at this low-residual pressure, the ratio of the specific heats γ is only slightly changed (in the range of 1.21–1.4), and thus its effect can be neglected. The pressure resulting from the LSD wave under the low-vacuum condition is estimated to be in the order of 3×10^6 Pa. Therefore under the atmospheric background pressure, the pressure exerted on the surface by the LSD wave is almost a factor of 35 higher than that in vacuum condition. The total time, τ_0, in which the LSD wave has momentum transfer to the surface can be estimated.

For the case of atmospheric background, $\tau_0=\dfrac{P_{2D}\tau_{2D}}{P_0}$, (6)

where P_{2D} is the pressure after the LSD wave evolves to a two-dimensional cylindrical wave, τ_{2D} is the time needed to make the LSD wave become this two-dimensional wave, and P_0 is the pressure of 1 atmosphere,

$$P_{2D}=p_D\left(\frac{\tau_p}{\tau_{2D}}\right)^{2/3}, \tag{7}$$

where τ_p is the width of the laser pulse, and

$$\tau_{2D}=\frac{2}{3V_D^{3/2}\tau_p^{1/2}}[D_s^{3/2}-(V_D\tau_p)^{3/2}]+\tau_p, \tag{8}$$

where D_s is the diameter of the laser spot. From Eqs. (4)–(8), it is obvious that the lifetime of the LSD wave, τ_0, depends on the ambient density ρ_0, i.e., depends on the pressure of the ambient background. For instance, under the experimental condition that we used, τ_0 is obtained to be 1.9×10^4 ns for ambient pressure of one atmosphere. But for the case of ambient pressure at 2.7 Pa, τ_0 is about 443 ns. These lifetime values of the LSD wave are in the same orders of the lifetimes of the Si ions in the plasma measured in this work for ablation at atmospheric pressure and at 2.7 Pa, respectively. This indicates that the lifetime of Si ions in the plasma is closely correlated with the lifetime of the LSD wave. The higher pressure and density environment provided by the LSD wave for the case of laser ablation in atmospheric background makes the collisions in the plasma be substantially enhanced. The enhanced collisions and the long lifetime of

the LSD wave in atmosphere lead to the higher emission intensity of the Si ions and the longer lifetime of the emission spectrum, as observed in the experiment.

Since the neutral Si atoms in the plasma have long spatial distribution in vacuum, they can arrive at the surface of the substrate in the early stage (short delay time). This should be partly responsible for the complicated composition frequently observed near the surface of the films prepared by PLD. If one could properly adjust the ambient gas species and the background pressure in the chamber during the deposition of SiC thin films, these incoming Si atoms flux might be controlled effectively. This subject is a challenge and worthy of further studies.

IV. CONCLUSION

We have investigated the temporal and spatial characteristics of Si atoms in the plasma produced by nanosecond pulsed laser ablated SiC crystal. In vacuum, the spatial profile of the well-isolated line at 633.19 nm emitted from Si atoms in the plasma extends from the target surface to a distance near the edge of the plume (16 mm). Although higher intensity and narrower distribution for the chosen spectral lines are observed at distance larger than 5mm, the electron temperature and density have maximum values around the distance of 2mm from the target surface. It is interesting that the spectral line of Si atoms at 633.19nm exists only in the early stage of the plasma evolution in vacuum. However, the signal at 633.19nm emitted from the Si atoms disappears in air environment due to the gas phase collision effects in air background. Moreover, the lifetime of Si ions (at 637.13 nm) increases from 430 ns in a low vacuum (2.7 Pa) to 1.428×10^4 ns in ambient air. This phenomenon is closely related to the pressure resulting from the LSD wave. Due to the short decay time and the long spatial distribution for the excited Si atoms in the plasma, the neutral Si atoms can arrive at the surface of the substrate in the early stage of the plasma expansion, resulting in Si agglomerate or particulate near the interface between the substrate and the film grown. This may have detrimental effect on the quality of the films prepared using PLD technique.

ACKNOWLEDGMENTS

This work was supported by the National Natural Science Foundation of China under Grant No. 10675075, the Natural Science Foundation of Shandong Province under Grant No.Y2007A02, and Excellent Middle Aged and Young Scientist Foundation of Shandong Province under Grant No. 2004BS05007.

[1] B. Wu, Appl. Phys. Lett. **93**, 101104 (2008).
[2] S. Gurlui, M. Agop, P. Nica, M. Ziskind, and C. Focsa, Phys. Rev. E **78**, 026405 (2008).
[3] B. Wu, Y. C. Shin, H. Pakhal, N. M. Laurendeau, and R. P. Lucht, Phys. Rev. E **76**, 026405 (2007).
[4] I. I. Beilis, Appl. Phys. Lett. **89**, 091503 (2006).
[5] S. S. Harilal, C. V. Bindhu, R. C. Issac, V. P. N. Nampoori, and C. P. G. Vallabhan, J. Appl. Phys. **82**, 2140 (1997).
[6] R. F. Z. Lizarelli, M. M. Costa, E. Carvalho-Filho, F. D. Nunes, and V. S. Bagnato, Laser Phys. Lett. **5**, 63 (2008).
[7] T. E. Itina, J. Hermann, P. Delaporte, and M. Sentis, Phys. Rev. E **66**, 066406 (2002).
[8] X. Fu and H. Guo, Phys. Rev. E **65**, 067401 (2002).
[9] K. A. Pestka, J. D. Maynard, D. Gao, and C. Carraro, Phys. Rev. Lett. **100**, 055503 (2008).
[10] A. Gali, Phys. Rev. B **73**, 245415 (2006).
[11] N. A. Riza and M. Sheikh, Opt. Lett. **33**, 1129 (2008).
[12] C. Long, S. A. Ustin, and W. Ho, J. Appl. Phys. **86**, 2509 (1999).
[13] C. Y. Tang, F. H. Li, R. Wang, J. Zou, X. H. Zheng, and J. W. Liang, Phys. Rev. B **75**, 184103 (2007).
[14] Q. Cheng, S. Xu, J. Long, and K. Ostrikov, Appl. Phys. Lett. **90**, 173112 (2007).
[15] A. E. Rider, I. Levchenko, and K. Ostrikov, J. Appl. Phys. **101**, 044306 (2007).
[16] Y. Sun and T. Miyasato, J. Appl. Phys. **84**, 2602 (1998).
[17] M. J. Ying, Y. Y. Xia, Y. M. Sun, Q. M. Lu, M. W. Zhao, Y. C. Ma, X. D. Liu, and P. J. Liu, Appl. Surf. Sci. **207**, 227 (2003).
[18] J. Gordillo-vazquez, A. Perea, J. A. Chaos, J. Gonzalo, and C. N. Afonso, Appl. Phys. Lett. **78**, 7 (2001).
[19] W. L. Wiese and G. A. Martin, *Atomic Transition Probabilities* (National Stand, Washington, 1969).
[20] I. I. Beilis, Laser Part. Beams **25**, 53 (2007).
[21] A. De Giacomo, M. Dell'Aglio, R. Gaudiuso, G. Cristoforetti, S. Legnaioli, V. Palleschi, and E. Tognoni, Spectrochim. Acta, Part B **63**, 980 (2008).
[22] G. Bekfi, *Principles of Laser Plasmas* (Wiley, New York, 1976).
[23] A. N. Pirri, Phys. Fluids **16**, 1435 (1973).
[24] L. R. Hettche, T. R. Tucker, J. T. Schriempy, R. L. Stegman, and S. A. Metz, J. Appl. Phys. **47**, 1415 (1976).
[25] Y. Y. Xia, Q. P. Wang, L. M. Mei, C. Y. Tan, S. B. Yue, B. Z. Xu, and X. D. Liu, J. Phys. D **24**, 1933 (1991).